

Experimental Results Using a Low-Energy Focussed Ion Beam Column With Minimised Coulomb Interaction

Karin Marianowski and Erich Plies

Institute of Applied Physics, University of Tübingen, Tübingen, Germany.

Focussed ion beam (FIB) instruments are well established in many areas, e.g. inspection, repair and modification of integrated circuits and lithography masks, beam assisted etching, deposition as well as transmission electron microscopy (TEM) sample preparation. Most of these instruments are equipped with a Gallium liquid metal ion source (Ga-LMIS) and designed for high energy operation, i.e. for landing energies of 5 to 30 keV. However, high energy Gallium ions inevitably lead to removal of deposited material as well as to sample damage as amorphisation and implantation of Gallium. Hence, it is very desirable to have an instrument which enables landing energies of 3, 2 or even 1 keV without a considerable loss of neither resolution nor ion beam current. For this reason a completely new dedicated low-energy FIB system based on immersion optics has been designed, built and tested.

By now several laboratory low-energy focussed ion beam (LEFIB) systems have been built. In most systems the positive charged ions are retarded between the last electrode of the objective lens and the target by setting the target on high positive potential. With such a system very small probe sizes can be realised, see e.g. [1-6]. However, as a non-free-standing target brings along some disadvantages as a suppressed electron signal also systems with field-free as well as grounded target have been developed, see e.g. [7-11]. Since the results obtained in [11] are very promising, our enhanced approach is composed of the ideas presented there and the following new aspects:

- doubling of the ground related drift space voltage U_{DS} (booster voltage) to values up to -10 kV for a shorter interaction time,
- realisation of the optically favourable internal acceleration mode for both lenses [12],
- integration of an adjustable and changeable aperture for better alignment,
- pre-lens deflection for a smaller working distance (two deflector stages, eight electrodes per stage),
- reduction of the final energy E to 1 keV,
- implementation of an additional electrode for an improved electron signal (Figure 7).

The resulting distribution of the kinetic axial potential Φ as well as a schematic outline of the new LEFIB system are shown in Figure 1.

To be able to design an improved LEFIB system, the questions below have to be answered:

- Is the probe size dominated by the length of the drift space or by the working distance d_w ?
- Is the probe size dominated by the operation mode of the two lenses or by the kinetic axial potential of the drift space?
- How can the simulation approach be further enhanced?
- Which configuration of the LEFIB system (incorporating the operation modes of the two lenses, the working distance, the total system length, the lateral magnification as well as the diameter of the aperture) gives the best result for a final energy of 1, 2 and 3 keV?

The first two questions have already been answered in [13]: Most important is a short working distance and a high potential of the drift space, even though a short total system length and the internal acceleration mode of both lenses have a positive influence, too. To investigate the last two questions the

software packages OPTICS and IMAGE [14] were used: OPTICS for calculating basic optical properties of a given system configuration, IMAGE for investigating the influence of Coulomb interactions.

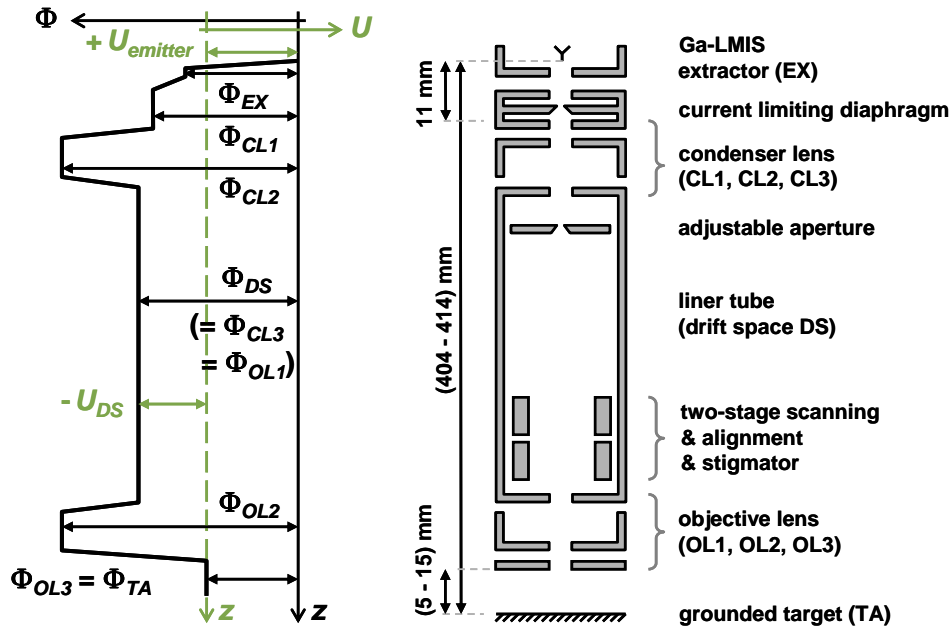


Figure 1. Schematic distribution of the kinetic axial potential Φ and the ground related voltage U together with a schematic outline of the new LEFIB system. The axial ray path is approximately telecentric between the two immersion lenses (not shown).

As can be seen from Figure 2 the large current $I_{emission}$ upstream the aperture has a major influence on the probe size. Hence, the current limiting effect of the aperture has to be considered in the simulation approach, too. As a consequence optimisation of the system configuration implies optimisation of lateral magnification M as well as aperture diameter $d_{aperture}$.

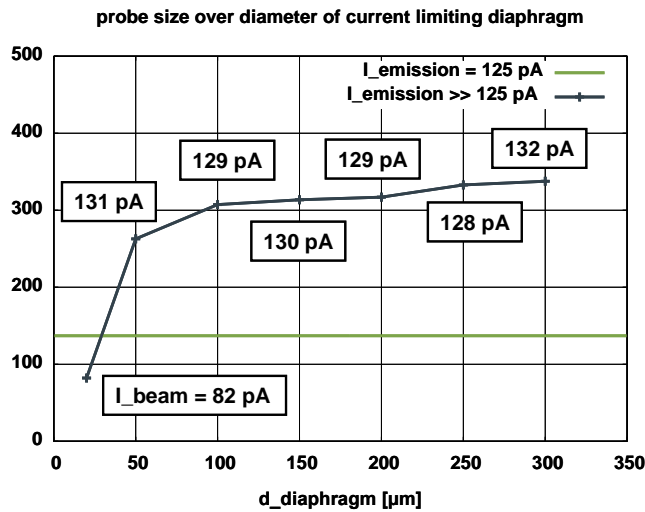


Figure 2. Dependency of the probe size d_{FW50} on the current upstream the aperture given by the diameter $d_{diaphragm}$ of the current limiting diaphragm. It is $I_{emission} \approx 18$ nA for $d_{diaphragm} = 300$ μm . The aperture diameter $d_{aperture}$ is 50 μm .

There are eight possible operation modes of a LEFIB system consisting of two immersion lenses and based on the booster principle, i.e. with the drift space set to high potential (see Figure 3). All of these modes have to be investigated to be able to answer the last question.

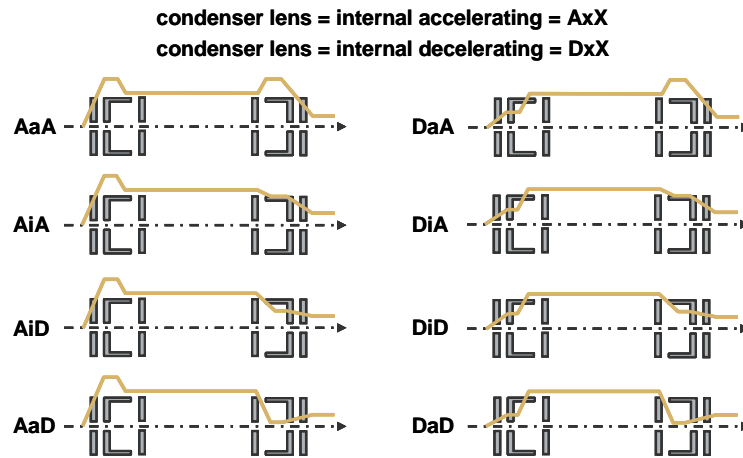


Figure 3. Possible operation modes of a LEFIB system consisting of two immersion lenses. xX depends on the operation mode of the objective lens and stands for aA, iA, iD or aD.

For a diameter of the current limiting diaphragm of $100\ \mu\text{m}$, i.e. $I_{\text{emission}} \approx 1.8\ \text{nA}$, aperture diameters between 40 and $200\ \mu\text{m}$ were investigated. As an example the results for an aperture diameter of $70\ \mu\text{m}$ and a final energy of $2\ \text{keV}$ are shown in Figures 4 and 5. The characteristics of the optimum system configurations for a beam current downstream the aperture of $125\ \text{pA}$ are listed in the left table of Table 1. Additionally, the results obtained with OPTICS are given in the right table. For the latter the probe size was calculated using the RPS algorithm presented in [15]. Comparing the results obtained with OPTICS and those obtained with IMAGE it becomes obvious that in case that Coulomb interactions are dominant the ray path between the two lenses has to be more divergent, i.e. a smaller $|M|$, than in the case that interactions can be neglected. For a $30\ \text{keV}$ FIB column with two einzel lenses and a crossover in between this rule was already mentioned in [16]. For more details on the simulations presented here see [17].

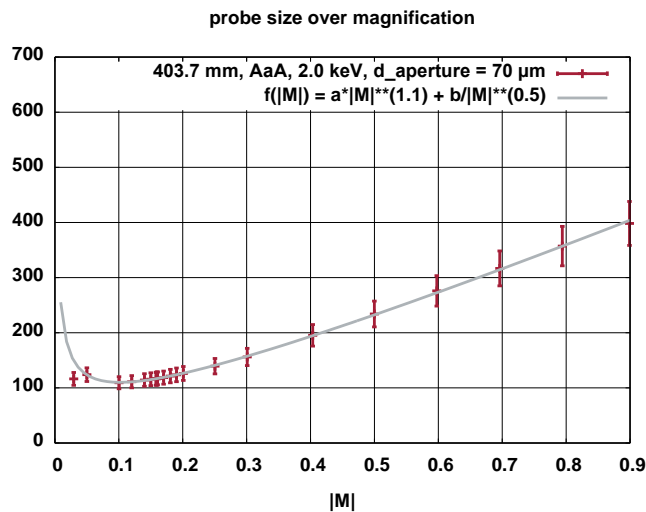


Figure 4. Dependency of the probe size d_{FW50} on the lateral magnification $|M|$ for $d_{\text{aperture}} = 70\ \mu\text{m}$ and $E = e\Phi_{TA} = 2\ \text{keV}$.

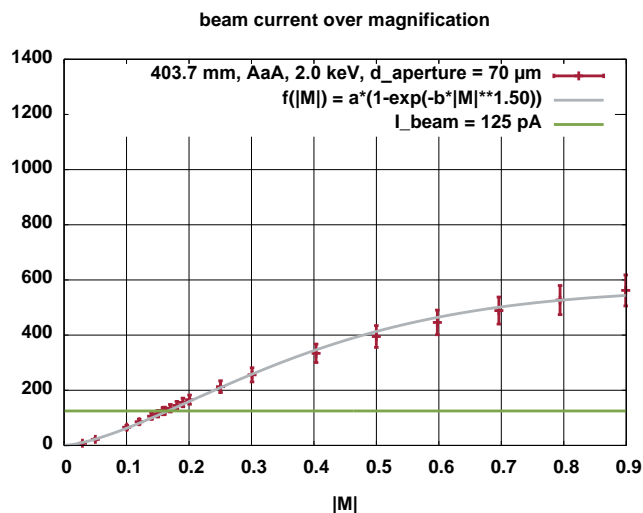


Figure 5. Dependency of the beam current I_{beam} downstream the aperture on the lateral magnification $|M|$ for $d_{aperture} = 70 \mu\text{m}$ and $E = 2 \text{ keV}$.

L_{system} [mm]	E [keV]	mode of operation	Φ_{DS} [kV]	$d_{aperture}$ [μm]	d_{FW50} [μm]	M
403.7	1.0	AiA	11.0	60	0.199	-0.27
403.7	2.0	AaA	12.0	60	0.113	-0.21
403.7	3.0	AaA	13.0	70	0.082	-0.15

L_{system} [mm]	E [keV]	mode of operation	Φ_{DS} [kV]	$d_{aperture}$ [μm]	d_{RPS} [μm]	M
403.7	1.0	AiA	11.0	-	0.058	-0.78
403.7	2.0	AaA	12.0	-	0.035	-0.46
403.7	3.0	AaA	13.0	-	0.026	-0.35

Table 1. Optimum system configurations obtained with IMAGE (left table) and obtained with OPTICS (right table) for $d_w = 5.0 \text{ mm}$, $I_{beam} = 125 \text{ pA}$ and $I_{probe} = I_{beam} / 2 = 63 \text{ pA}$.

Figures 6 and 7 are engineering drawings of two key units of the column. Since the liner tube is on high negative voltage U_{DS} the valve disc of the vacuum valve, the aperture as well as its support have to be on high voltage, too (Figure 6). Furthermore, a high liner tube voltage requires that the voltages for alignment, scanning and astigmatism correction are superimposed on this high voltage (Figure 7). As the objective lens is operated in the internal acceleration mode a special insulator design with a sufficient creepage path is implemented. The experimental setup of the complete LEFIB column is shown in Figure 8.

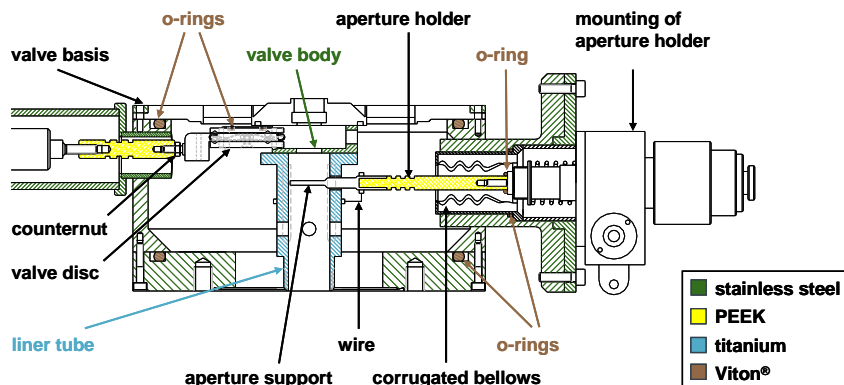


Figure 6. Cross-sectional view of the column unit containing the vacuum valve and the adjustable aperture. The inner diameter of the liner tube is 18 mm.

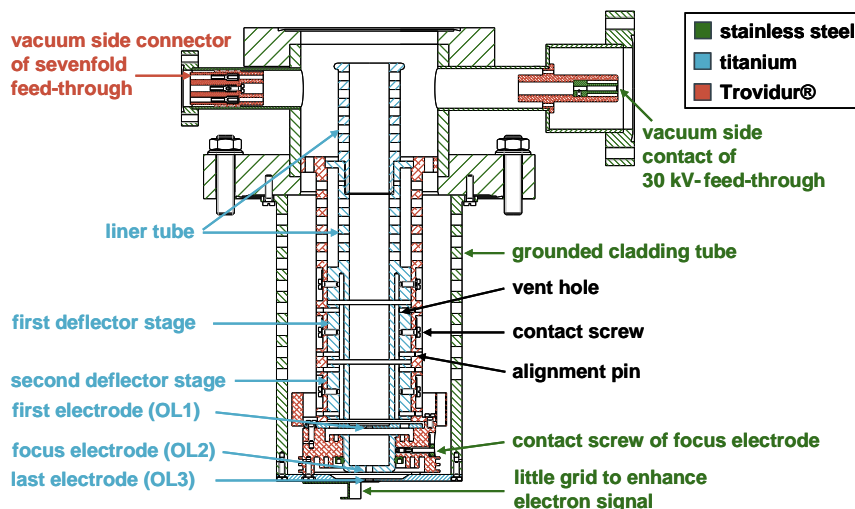


Figure 7. Cross-sectional view of the column unit containing the two-stage scanning deflector and the objective lens. The two stages of the scanning deflector are also used for alignment and the second stage serves as stigmator, too. The inner diameter of the liner tube is 18 mm.

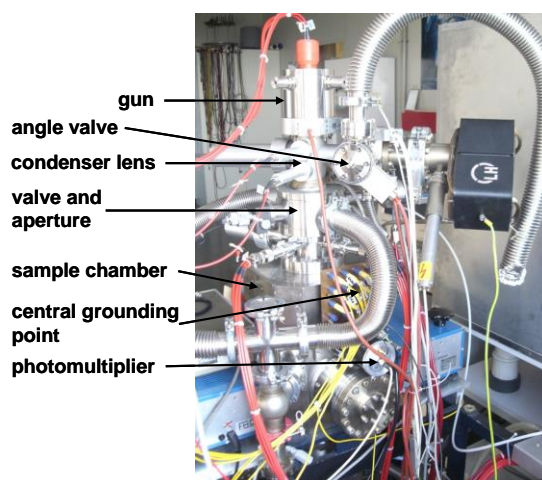


Figure 8. Back view of the experimental setup of the new LEFIB system. The total system length, i.e. the distance between emitter tip and target, is 404 mm.

E [keV]	U_{DS} [kV]	d_w [mm]	$d_{aperture}$ [μm]	I_{beam} [pA]	d_{FW50} [nm]	Δd_{FW50} [nm]
1.0	-10.00	5.0	70	(457)	(700)	(100)
2.0	-10.00	5.0	70	300	455	60
3.0	-10.00	5.0	70	(471)	(250)	(50)

Table 2. Experimental results obtained with the knife edge method (12% - 88%) and a Faraday cup. The specimen used is a Quantifoil[®] S 7/2 [18] lying on a 400 copper mesh. Values in brackets are estimates from the electron signal (Figure 9) and simulations, respectively. For more details see the text.

In the case of a final energy of $E = 2$ keV experimental results for the probe diameter d_{FW50} and the beam current $I_{beam} = 2 I_{probe}$ are obtained with the knife edge method and a Faraday cup, see Table 2. Due to a subsequent breakdown of the sample stage the electron signal and image interpretation are used

for $E = 1$ and 3 keV to obtain the probe diameter, see Table 2 and Figure 9. The ion beam current is estimated from simulations, see Table 2. For more details on the experimental results, which are in good agreement with the simulation results, see [17].

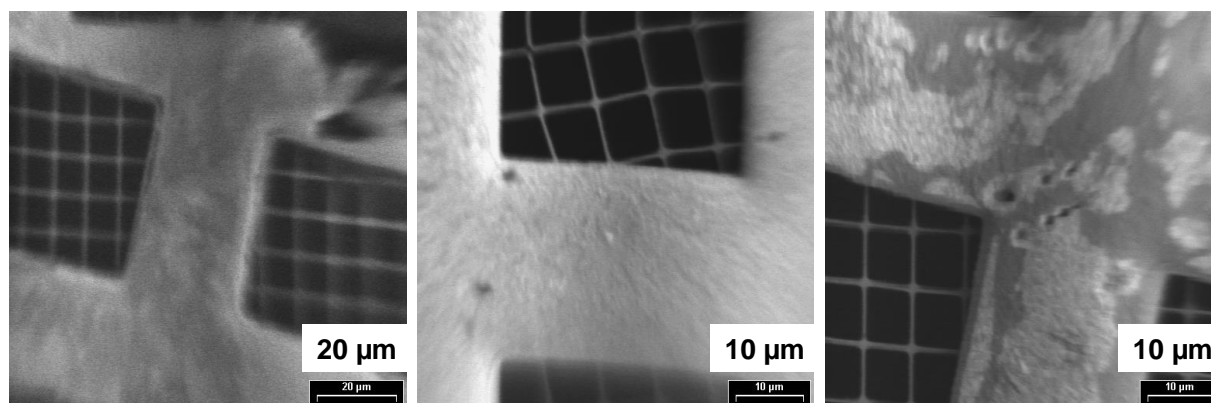


Figure 9. Electron signal for $U_{DS} = -10$ kV, $d_w = 5$ mm, $E = 1$ keV (left), $E = 2$ keV (mid) and $E = 3$ keV (right), respectively. Fine grid width ≈ 0.5 μm .

A completely new LEFIB system has been designed, built and tested for final energies between 1 and 3 keV. Due to an improved design based on an enhanced simulation approach including the large current upstream the aperture, i.e. due to a more realistic and more complete calculation of Coulomb interactions, and by optimising the aperture diameter as well as the lateral magnification the new LEFIB system exhibits the best performance triple E , I_{probe} , d_{FW50} presented in literature for systems with free-standing target so far [19].

References:

- [1] DH Narum and RFW Pease, *J. Vac. Sci. Technol. B* **6** (1988), p. 966.
- [2] H Kasahara *et al*, *J. Vac. Sci. Technol. B* **6** (1988), p. 974.
- [3] H Sawaragi *et al*, *J. Vac. Sci. Technol. B* **8** (1990), p. 1848.
- [4] S Nagamachi *et al*, *Appl. Phys. Lett.* **62** (1993), p. 2143.
- [5] J Yanagisawa *et al*, *J. Vac. Sci. Technol. B* **13** (1995), p. 2621.
- [6] PW Nebiker *et al*, *Nucl. Instr. Meth. B* **113** (1996), p. 205.
- [7] J Orloff, *Microel. Engin.* **6** (1987), p. 327.
- [8] W Driesel, *Ultramicroscopy* **52** (1993), p. 65.
- [9] T Chikyow *et al*, *Surf. Sci.* **386** (1997), p. 254.
- [10] P Gnauck, dissertation, Tübingen, 2000.
- [11] M Rauscher, dissertation, Tübingen, 2006.
- [12] K Marianowski, diploma thesis, Tübingen, 2006.
- [13] K Marianowski *et al*, *Nucl. Instr. Meth. A* **645** (2011), p. 116.
- [14] Software by Mebs Ltd., London, www.mebs.co.uk
- [15] JE Barth and P Kruit, *Optik* **101** (1996), p. 101.
- [16] P Kruit and XR Jiang, *J. Vac. Sci. Technol. B* **14** (1996), p. 1635.
- [17] K Marianowski, dissertation, Tübingen, 2014.
- [18] www.quantifoil.com
- [19] Many thanks go to Dr. Lothar Bischoff of the FZ Rossendorf for the supply of the gallium LMIS. Funding of part of this work by Bal-TEC AG, Principality of Liechtenstein, is gratefully acknowledged.